Polymer 54 (2013) 1072–1079

Contents lists available at SciVerse ScienceDirect

Polymer

journal homepage: www.elsevier.com/locate/polymer

Synthesis of Donor–Acceptor polymers through control of the chemical structure: Improvement of PCE by planar structure of polymer backbones

Ho Jun Song [a], Tae Ho Lee [a], Myung Hee Han [a], Jang Yong Lee [b], Doo Kyung Moon [a,*]

[a] Department of Materials Chemistry and Engineering, Konkuk University, 1 Hwayang-dong, Gwangjin-gu, Seoul 143-701, Republic of Korea
[b] Energy Materials Research Center, Korea Research Institute of Chemical Technology, P.O. Box 107, Yuseong, Daejeon 305-600, Republic of Korea

ARTICLE INFO

Article history:
Received 30 August 2012
Received in revised form
16 October 2012
Accepted 21 October 2012
Available online 9 November 2012

Keywords:
Quinoxaline
OPVs
Conjugated polymer

ABSTRACT

A new acceptor unit with high solubility octyloxy-diphenylquinoxaline was synthesized with octyloxy-dibenzophenazine. The new D–A type polymers poly(carbazole-octyloxy diphenylquinoxaline) (PCzPDTQ) and octyloxy-dibenzophenazine) (PCzFDTQ), which adopted carbazole as a donor, were polymerized through a Suzuki coupling reaction. PCzPDTQ and PCzFDTQ dissolved in organic solvents and showed high thermal stability. Due to the appropriate LUMO energy levels, an effective charge transport and a low band gap (2.06 and 1.97 eV) were observed in PCzPDTQ and PCzFDTQ. According to X-ray diffraction measurements, a single broad diffraction peak was detected at approximately 20.5°. The π–π stacking distances (d_π) for PCzPDTQ and PCzFDTQ were 4.4 and 4.3 Å, respectively. When PCzPDTQ and $PC_{71}BM$ were blended in a 1:3 ratio, The open-circuit voltage (V_{OC}), short-circuit current (J_{SC}), fill factor (FF) and power conversion efficiency (PCE) were 0.85 V, 6.5 mA/cm^2, 32.2% and 1.8%, respectively. The efficiency of PCzFDTQ tended to improve as $PC_{71}BM$ increased. At a 1:6 ratio of PCzFDTQ to $PC_{71}BM$, V_{oc}, J_{sc}, FF and PCE were 0.85 V, 5.5 mA/cm^2, 44.9% and 2.1%, respectively. In terms of FF, 39% of the increase was observed in PCzFDTQ.

1. Introduction

For several decades, semiconducting polymers have been used in diverse applications, such as organic light emitting diodes (OLEDs) [1–4], organic photovoltaic cells (OPVs) [5–11] and organic thin film transistors (OTFTs) [12,13]. In these applications, OPVs have drawn great attention with the global technology trend toward economic feasibility and continuous development, while preserving the environment. Low power conversion efficiency (PCE) has been the largest obstacle in developing OPVs [6]. For the past few years, the Donor–Acceptor (D–A) type low-band gap polymer has drawn great attention, as its electronic properties can be easily be changed based on the unique combination of the D–A unit. This polymer can also increase the absorption spectra with long wavelengths.

Among the D–A polymer acceptor units, quinoxaline derivatives have been widely used due to the electro-withdrawing properties of the two imine nitrogens. Quinoxaline derivatives can be easily structurally deformed with high solubility. In addition, its electronic properties can be changed with various substituents [14,15]. Most D–A polymers, which used quinoxaline derivatives, demonstrate low efficiency (2–3%) because of the non-planar properties of the two phenyl rings [16,17]. Recently, the Jen group reported that with the two phenyl rings connected to the single bond between ortho-positions, the PCE improved from 5.69% up to 6.24% [18]. These fused-phenyl rings can enhance the efficiency through a reduction of the energetic disorder of the polymer after facilitating polymer coplanarity and interchain π–π interactions [7,8,14]. In these fused-phenyl rings, however, it is difficult to introduce the akyl-chains necessary to become highly soluble.

Recently, alkoxy-benzothiadizole derivatives, for which flexible alkoxy-chains were introduced at the 5th and 6th positions, have been reported [19,20]. These kinds of alkoxy-benzothiadizole derivatives have a high solubility with the absorption spectra and electronic properties of benzothiadiazole. Alkoxy-chains with good solubility introduced at the 11th and 12th positions of the dibenzophenazine derivatives, which are quinoxaline derivatives with a fused-phenyl ring similar to an alkoxy-benzothiadizole, may produce polymers with a high solubility along with the absorption spectra and coplanarity properties of the dibenzo-phenazine derivates.

In this study, new acceptor units with a high solubility, 5,8-bis(5-bromothiophen-2-yl)-6,7-bis(octyloxy)-2,3-diphenylquinoxaline and

* Corresponding author. Tel.: +82 2 450 3498; fax: +82 2 444 0765.
E-mail address: dkmoon@konkuk.ac.kr (D.K. Moon).

0032-3861/$ – see front matter © 2013 Elsevier Ltd. All rights reserved.
http://dx.doi.org/10.1016/j.polymer.2012.10.056

10,13-bis(5-bromothiophen-2-yl)-11,12-bis(octyloxy)dibenzo[a,c] phenazine, were synthesized. Two new D–A type polymers, poly(carbazole-octyloxy diphenylquinoxaline) (PCzPDTQ) and poly(carbazole-octyloxydibenzophenazine) (PCzFDTQ), in which carbazole derivatives were introduced as a donor, were successfully polymerized. Compared with PCzPDTQ, a more effective π–π interaction is expected in PCzFDTQ because of the superior coplanarity properties of fused-phenyl rings, which enables high FF in OPVs.

2. Experimental section

2.1. Instruments and characterization

Unless otherwise specified, all reactions were carried out under a nitrogen atmosphere. Solvents were dried using standard procedures. All column chromatography was performed with silica gel (230–400 mesh, Merck) as the stationary phase. ^{1}H NMR spectra were performed in a Bruker ARX 400 spectrometer using solutions in $CDCl_3$ with chemical shifts recorded in ppm units using TMS as the internal standard. The elemental analyses were measured with EA1112 using a CE Instrument. Electronic absorption spectra were measured in chloroform using an HP Agilent 8453 UV–Vis spectrophotometer. The cyclic voltammetric waves were produced using a Zahner IM6eX electrochemical workstation with a 0.1 M acetonitrile (purged with nitrogen for 20 min) solution containing tetrabutylammonium hexafluorophosphate (Bu_4NPF_6) as the electrolyte at a constant scan rate of 50 mV/s. ITO, a Pt wire, and silver/silver chloride [Ag in 0.1 M KCl] were used as the working, counter, and reference electrodes, respectively. The electrochemical potential was calibrated against Fc/Fc^+. The HOMO levels of the polymers were determined using the oxidation onset value. Onset potentials are values obtained from the intersection of the two tangents drawn at the rising current and the baseline changing current of the CV curves. TGA measurements were performed on an NETZSCH TG 209 F3 thermogravimetric analyzer. All GPC analyses were made using THF as an eluent and a polystyrene standard as a reference. Powder X-ray diffraction (XRD) patterns were obtained using a Bruker D2Phaser(LynxEye of 1D detector) with CuKα (1.54 Å) radiation. Topographic images of the active layers were obtained through atomic force microscopy (AFM) in a tapping mode under ambient conditions using an XE-100 instrument. Theoretical analyses were performed using density functional theory (DFT), as approximated by the B3 LYP functional and employing the 6–31G* basis set in Gaussian09.

2.2. Fabrication and characterization of polymer solar cells

All of the bulk-heterojunction PV cells were prepared using the following device fabrication procedure. The glass/indium tin oxide (ITO) substrates [Sanyo, Japan (10 Ω/γ)] were sequentially lithographically patterned, cleaned with detergent, and ultrasonicated in deionized water, acetone, and isopropyl alcohol. The substrates were then dried on a hot plate at 120 °C for 10 min and treated with oxygen plasma for 10 min to improve the contact angle immediately before the film coating process. Poly(3,4-ethylenedioxythiophene): poly(styrene-sulfonate) (PEDOT:PSS, Baytron P 4083 Bayer AG) was passed through a 0.45-μm filter before being deposited onto the ITO at a thickness of ca. 32 nm by spin-coating at 4000 rpm in air and then dried at 120 °C for 20 min inside a glove box. Composite solutions with polymers and PCBM were prepared using 1,2-dichlorobenzene (DCB). The concentration was controlled adequately in the 0.5 wt% range. The solutions were then filtered through a 0.45-μm PTFE filter and then spin-coated (500–2000 rpm, 30 s) on top of the PEDOT:PSS layer. The device fabrication was completed by depositing thin layers of BaF_2 (1 nm), Ba (2 nm), and Al (200 nm) at pressures of less than 10^{-6} torr. The active area of the device was 4.0 mm^2. Finally, the cell was encapsulated using a UV-curing glue (Nagase, Japan). In this study, all of the devices were fabricated with the following structure: ITO glass/PEDOT:PSS/polymer:PCBM/BaF_2/Ba/Al/encapsulation glass.

The illumination intensity was calibrated using a standard a Si photodiode detector that was equipped with a KG-5filter. The output photocurrent was adjusted to match the photocurrent of the Si reference cell to obtain a power density of 100 mW/cm^2. After the encapsulation, all of the devices were operated under an ambient atmosphere at 25 °C. The current–voltage (I–V) curves of the photovoltaic devices were measured using a computer-controlled Keithley 2400 source measurement unit (SMU) that was equipped with a Peccell solar simulator under an illumination of AM 1.5G (100 mW/cm^2). The thicknesses of the thin films were measured using a KLA Tencor Alpha-step 500 surface profilometer with an accuracy of 1 nm.

2.3. Synthesis

All reagents were purchased from Aldrich, Acros or TCI companies. All chemicals were used without further purification. The following compounds were synthesized following modified literature procedures: 4,7-dibromo-5,6-bis(octyloxy)benzo[c] [1,2,5]thiadiazole [20], 9-(heptadecan-9-yl)-2,7-bis(4,4,5,5-tetramethyl-1,3,2-dioxaborolan-2-yl)-9H-carbazole [6].

2.4. 5,8-dibromo-6,7-bis(octyloxy)-2,3-diphenylquinoxaline

Under a nitrogen atmosphere, 4,7-dibromo-5,6-bis(octyloxy) benzo[c] [1,2,5]thiadiazole (4.0 g, 7.27 mmol) and zinc (5.88 g 90.0 mmol) dust were dissolved in 110 ml acetic acid. The mixture was refluxed for 3 h at 80 °C. After cooling to room temperature, the reaction mixture was washed with a NaOH solution. The solids that resulted after evaporation of the organic solvent and benzil (3.36 g, 15.92 mmol) were dissolved in 110 ml acetic acid. The mixture was refluxed for 1 day at 60 °C. After cooling to room temperature, an orange colored mixture was observed. After filtration, the reaction mixture was purified by column chromatography on silica gel (dichloromethane as eluent) to obtain the product as a green solid (3.2 g, 63.4%) ^{1}H NMR (400 MHz; $CDCl_3$; Me_4Si): 7.62(d, 4H; Ar) 7.37(m, 6H; Ar) 4.20(t, 4H; CH_2) 1.92(m, 4H; CH_2) 1.55(m, 4H; CH_2) 1.33(m, 16H; CH_2) 0.90(t, 6H; CH_3) ^{13}C NMR (100 MHz; $CDCl_3$; Me_4Si): 153.81; 152.69; 138.24; 137.14; 130.22; 129.25; 128.30; 117.26; 74.86; 31.88; 30.33; 29.45; 29.31; 26.07; 22.70; 14.13. Anal. Calcd for: $C_{36}H_{44}Br_2N_2O_2$: C, 62.07; H, 6.37; N, 4.02; O, 4.59 found: C, 61.20; H, 6.44; N, 3.92; O, 4.99.

2.5. 6,7-bis(octyloxy)-5,8-di(thiophen-2-yl)-2,3-diphenylquinoxaline

5,8-dibromo-6,7-bis(octyloxy)-2,3-diphenylquinoxaline 8 (2.0 g, 2.87 mmol) and tributyl(thiophen-2-yl)stannane (2.73 ml, 8.61 mmol) in toluene (75 ml) was added to $PdCl_2(PPh_3)_2$ (0.203 g 0.29 mmol) under a nitrogen atmosphere. After refluxing for 48 h at 80 °C, the mixture was cooled to room temperature and then poured into H_2O; the organic layer was extracted by $CHCl_3$ and dried over anhydrous Na_2SO_4. The crude product was purified by column chromatography on silica gel to give the product as an orange solid (1.5 g, 74.3%) ^{1}H NMR (400 MHz; $CDCl_3$; Me_4Si): 8.05 (d, 2H; Ar) 7.65(d, 4H; Ar) 7.55(d, 2H; Ar) 7.33(m, 6H; Ar) 7.20(d, 2H; Ar) 4.03(t, 4H; CH_2) 1.77(m, 4H; CH_2) 1.39(m, 4H; CH_2) 1.29(m, 16H; CH_2) 0.90(t, 6H; CH_3). ^{13}C NMR (100 MHz; $CDCl_3$; Me_4Si): 152.88; 150.24; 138.93;

136.43; 133.49; 130.88; 130.32; 128.66; 128.14; 127.85; 126.06; 124.19; 74.10; 31.87; 30.41; 29.50; 29.31; 26.07; 22.71; 14.15. Anal. Calcd for: $C_{44}H_{50}N_2O_2S_2$: C, 75.17; H, 7.17; N, 3.98; O, 4.55; S, 9.12 Found: C, 73.14; H, 7.35; N, 3.83; O, 5.13; S, 7.85.

2.6. 5,8-bis(5-bromothiophen-2-yl)-6,7-bis(octyloxy)-2,3-diphenylquinoxaline (M1)

Under a nitrogen atmosphere, 6,7-bis(octyloxy)-5,8-di(thiophen-2-yl)-2,3-diphenylquinoxaline (1.5 g, 2.13 mmol) was dissolved in 140 ml of THF, and then NBS (0.87 g, 4.9 mmol) was added in portions. The mixture was stirred for 24 h at room temperature. The mixture was then poured into water and extracted with chloroform. The combined organic layers were dried over Na_2SO_4, and the solvent was removed. The crude product was purified with column chromatography to give M1 as a red-orange solid (1.2 g, 65.5%) ^{1}H NMR (400 MHz; $CDCl_3$; Me_4Si): 7.97(d, 2H; Ar) 7.63(d, 4H; Ar) 7.36(m, 6H; Ar) 7.14(d, 2H; Ar) 4.07(t, 4H; CH_2) 1.83(m, 4H; CH_2) 1.42(m, 4H; CH_2) 1.30(m, 16H; CH_2) 0.90(t, 6H; CH_3). ^{13}C NMR (100 MHz; $CDCl_3$; Me_4Si): 152.68; 150.57; 138.46; 135.89; 135.19; 131.25; 130.33; 128.95; 128.89; 128.25; 123.35; 116.09; 74.22; 31.85; 30.42; 29.48; 29.30; 26.07; 22.70; 14.13. Anal. Calcd for: $C_{44}H_{48}Br_2N_2O_2S_2$: C, 61.39; H, 5.62; N, 3.25; O, 3.72; S, 7.45 Found: C, 61.23; H, 5.65; N, 3.13; O, 4.28; S, 7.42.

2.7. 10,13-dibromo-11,12-bis(octyloxy)dibenzo[a,c]phenazine

Under a nitrogen atmosphere, 4,7-dibromo-5,6-bis(octyloxy) benzo[c] [1,2,5]thiadiazole (1.75 g, 3.18 mmol) and zinc (2.58 g 39.4 mmol) dust were dissolved in 110 ml acetic acid. The mixture was refluxed for 3 h at 80 °C. After cooling to room temperature, the reaction mixture was washed with a NaOH solution. The solids that resulted after the evaporation of the organic solvent and 9,10-phenanthrenequinone (1.46 g, 7.0 mmol) were dissolved in 110 ml acetic acid. The mixture was refluxed for 1 day at 60 °C. After cooling to room temperature, an orange colored mixture was observed. After filtration, the reaction mixture was purified by column chromatography on silica gel (dichloromethane as eluent) to obtain the product as a light-yellow solid (1.3 g, 58.9%) ^{1}H NMR (400 MHz; $CDCl_3$; Me_4Si): 9.29 (d, 2H; Ar) 8.41 (t, 2H; Ar) 7.68 (m, 4H; Ar) 4.27(t, 4H; CH_2) 1.96(t, 4H; CH_2) 1.59(m, 4H; CH_2) 1.42(m, 16H; CH_2) 0.91(t, 6H; CH_3). ^{13}C NMR (100 MHz; $CDCl_3$; Me_4Si): 153.91; 141.80; 137.92; 132.00; 130.49; 129.47; 127.96; 126.71; 122.73; 117.21; 74.94; 31.90; 30.41; 29.50; 29.35; 26.12; 22.72; 14.14. Anal. Calcd for: $C_{36}H_{42}Br_2N_2O_2$: C, 62.26; H, 6.10; N, 4.03; O, 4.61 Found: C, 60.16; H, 5.78; N, 3.79; O, 5.11.

2.8. 11,12-bis(octyloxy)-10,13-di(thiophen-2-yl)dibenzo[a,c] phenazine

10,13-dibromo-11,12-bis(octyloxy)dibenzo[a,c]phenazine (1.0 g, 1.44 mmol) and trimethyl(thiophen-2-yl)stannane (1.35 ml, 4.3 mmol) in toluene (37 ml) was added to $PdCl_2(PPh_3)_2$ (0.101 g 0.15 mmol) under a nitrogen atmosphere. After refluxing for 48 h at 80 °C, the mixture was cooled to room temperature and then poured into H_2O; the organic layer was extracted by $CHCl_3$ and dried over anhydrous Na_2SO_4. The crude product was purified by column chromatography on silica gel to give the product as an orange liquid (0.6 g, 59.3%) ^{1}H NMR (400 MHz; $CDCl_3$; Me_4Si): 9.11 (d, 2H; Ar) 8.30 (t, 2H; Ar) 7.98 (t, 2H; Ar) 7.58(d, 2H; Ar) 7.53(m, 4H; Ar) 7.20(t, 2H; Ar) 3.98(t, 4H; CH_2) 1.72(m, 4H; CH_2) 1.34(m, 4H; CH_2) 1.21(m, 16H; CH_2) 0.82(t, 6H; CH_3). ^{13}C NMR (100 MHz; $CDCl_3$; Me_4Si): 153.10; 140.34; 138.02; 133.71; 131.89; 130.93; 130.44; 129.71; 127.85; 127.77; 127.10; 126.08; 124.26; 122.67; 74.21; 31.93; 30.51; 29.56; 29.37; 26.14; 22.76; 14.21.

2.9. 10,13-bis(5-bromothiophen-2-yl)-11,12-bis(octyloxy)dibenzo [a,c]phenazine (M2)

Under a nitrogen atmosphere, 11,12-bis(octyloxy)-10,13-di(thiophen-2-yl)dibenzo[a,c]phenazine 12 (0.3 g 0.427 mmol) was dissolved in 30 ml of THF, and NBS (0.174 g, 0.982 mmol) was then added in portions. The mixture was stirred for 24 h at room temperature. Then, the mixture was poured into water and extracted with chloroform. The combined organic layers were dried over Na_2SO_4, and then the solvent was removed. The crude product was purified with column chromatography to give M2 as a red liquid (0.24 g 65.4%) ^{1}H NMR (400 MHz; $CDCl_3$; Me_4Si): 9.10 (d, 2H; Ar) 8.31 (t, 2H; Ar) 7.90 (t, 2H; Ar) 7.60(d, 4H; Ar) 7.20(m, 2H; Ar) 3.98(t, 4H; CH_2) 1.72(m, 4H; CH_2) 1.34(m, 4H; CH_2) 1.21(m, 16H; CH_2) 0.82(t, 6H; CH_3) ^{13}C NMR (100 MHz; $CDCl_3$; Me_4Si): 152.75; 140.39; 137.18; 135.21; 131.88; 131.26; 130.03; 029.87; 128.94; 127.83; 127.14; 123.29; 122.62; 115.74; 74.23; 31.91; 30.54; 29.73; 29.55; 29.37; 26.15; 22.75; 14.18.

2.10. Poly[carbazole-alt-dithienyl-diphenylquinoxaline] (PCzPDTQ)

9-(heptadecan-9-yl)-2,7-bis(4,4,5,5-tetramethyl-1,3,2-dioxaborolan-2-yl)-9H-carbazole (0.25 g, 0.29 mmol), M1 (0.191 g, 0.29 mmol), $Pd(PPh_3)_4(0)$ (0.009 g, 0.008 mmol) and Aliquat336, were placed in a Schlenk tube, purged with three nitrogen/vacuum cycles, and under a nitrogen atmosphere, added 2 M degassed aqueous K_2CO_3 (10 ml) and dry toluene (20 ml). The mixture was heated to 90 °C and stirred in the dark for 48 h. After the polymerization was complete, it was end-capped with bromothiophene. After reaction quenching, the whole mixture was poured into methanol. The precipitate was filtered off, purified with a Soxhlet extraction in the following order: methanol, acetone and chloroform. The polymer was recovered from the chloroform fraction and precipitated into methanol. The final product was obtained after drying in vacuum. Dark red solid (0.24 g 73.2%). ^{1}H NMR (400 MHz; $CDCl_3$; Me_4Si): $\delta = 8.24–8.11$ (m), 7.93–7.38 (m), 4.70 (s, 1H), 4.19 (d, 4H), 2.46 (br, 2H), 2.04–1.93 (m), 1.36–1.14 (m), 0.88–0.75 (m). Anal. Calcd for: $C_{73}H_{91}N_3O_2S_2$: C, 79.23; H, 8.29; N, 3.80; O, 2.89; S, 5.79. Found: C, 76.39; H, 8.21; N, 3.58; O, 2.50; S, 5.58.

2.11. Poly[carbazole-alt-dithienyl-dibenzophenazine] (PCzFDTQ)

9-(Heptadecan-9-yl)-2,7-bis(4,4,5,5-tetramethyl-1,3,2-dioxaborolan-2-yl)-9H-carbazole (0.25 g, 0.29 mmol), M2 (0.184 g 0.28 mmol), $Pd(PPh_3)_4(0)$ (0.009 g, 0.008 mmol) and Aliquat336 were placed in a Schlenk tube, purged with three nitrogen/vacuum cycles, and 2 M degassed aqueous K_2CO_3 (10 ml) and dry toluene (20 ml) were added under a nitrogen atmosphere. The mixture was heated to 90 °C and stirred in the dark for 48 h. After the polymerization was complete, it was end-capped with bromothiophene. After reaction quenching, the whole mixture was poured into methanol. The precipitate was filtered off, purified with a Soxhlet extraction in the following order: methanol, acetone and chloroform. The polymer was recovered from the chloroform fraction and precipitated into methanol. The final product was obtained after drying under vacuum. Dark black solid (0.23 g 72.1%). ^{1}H NMR (400 MHz; $CDCl_3$; Me_4Si): $\delta = 9.56$ (s, 2H), 8.64–8.63 (s, 2H), 8.25–8.05 (m), 7.88–7.69 (m), 4.75 (s, 1H), 4.23–4.22 (d, 4H), 2.50 (br, 2H), 2.08–1.94 (m), 1.36–1.12 (m), 0.88–0.72 (m). Anal. Calcd for: $C_{73}H_{89}N_3O_2S_2$: C, 79.37; H, 8.12; N, 3.80; O, 2.90; S, 5.81. Found: C, 79.03; H, 8.20; N, 3.80; O, 2.09; S, 5.49.

3. Results and discussion

Scheme 1 shows the chemical structure and the synthesis process. 6,7-bis(octyloxy)-5,8-di(thiophen-2-yl)-2,3-diphenylquinoxaline was

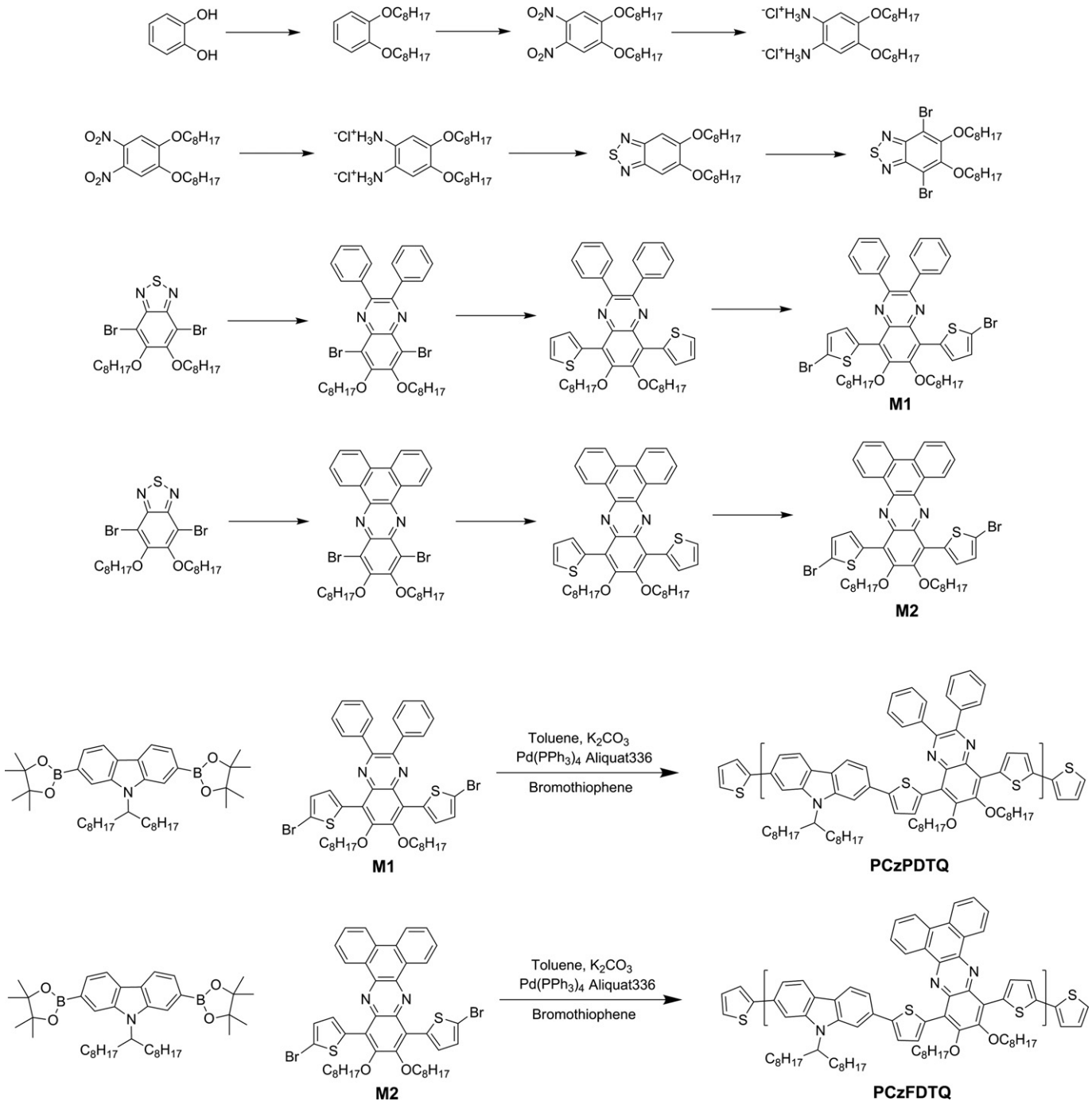

Scheme 1. Scheme of monomer synthesis and polymerization.

synthesized using tributyl(thiophen-2-yl)stannane and $PdCl_2(PPh_3)_2$. However, 11,12-bis(octyloxy)-10,13-di(thiophen-2-yl)dibenzo[a,c] phenazine wasn't synthesized using tributyl(thiophen-2-yl)stannane and various catalysts. Finally, 11,12-bis(octyloxy)-10,13-di(thiophen-2-yl)dibenzo[a,c]phenazine was successfully synthesized using trimethyl(thiophen-2-yl)stannane and $PdCl_2(PPh_3)_2$. This result might be caused by strong steric hindrance of fused-ring compared to separated phenyl-ring. As shown in this scheme, PCzPDTQ and PCzFDTQ were polymerized through the Suzuki coupling reaction using carbazole and the monomers M1, M2. The polymerization was reacted for 48 h at 90 °C using palladium catalysts (0), a 2 M potassium carbonate solution, aliquot 336 as a surfactant and toluene as a solvent. Upon completion, the polymer was end-capped with boromothiophene. The synthesized polymer was purified using a Soxhlet extractor with methanol, acetone and chloroform. The chloroform fraction was recovered. The polymerization rates were 73% and 72%, respectively. The polymers were dissolved with organic solvents, such as THF, chloroform, chlorobenzene and o-dichlorobenze, to produce both a homogenous and semi-transparent red film through spin-coating.

The molecular weights and thermal properties of the synthesized polymers are shown in Table 1. Using GPC with polystyrene as the standard, the number-average molecular weights (M_n) of PCzPDTQ and PCzFDTQ were determined to be 31.0 and 12.3 kg/mol, respectively. The polydispersity indices (PDI) showed very

Table 1
Molecular weight and thermal properties of the polymers.

Polymer	M_n (kg/mol)	M_w (kg/mol)	PDI	T_d (°C)
PCzPDTQ	31.0	52.2	1.68	339
PCzFDTQ	12.3	19.6	1.70	345

narrow distribution with 1.68 and 1.70. The degree of polymerization for PCzFDTQ was slightly lower than PCzPDTQ because dibenzophenazine has a rigid structure. With rigid backbone structure, polymerization becomes less effective [6]. According to a TGA thermal analysis, shown in Table 1, high thermal stabilities were observed at 339–345 °C (5 wt% loss). Due to a rigid phenazine structure, the thermal stability was slightly higher in PCzFDTQ, indicating a potential use in polymeric solar cells or other optoelectronic devices [21], which require high thermal stabilities at temperatures of 300 °C or higher.

Fig. 1 shows the UV–Vis spectra of the solution (10^{-5} M) and the thin film (50 nm) after spin coating. The solution maximum absorption wavelengths (λ_{max}) were 386 and 492 nm for PCzPDTQ and 395 and 513 nm for PCzFDTQ. Absorption spectra between 300 and 400 nm are caused by the $\pi-\pi^*$ transition of the conjugated backbone. Absorption spectra between 500 and 600 nm are caused by an intermolecular charge transfer between donor acceptors [14].

The maximum absorption wavelengths of the thin film (λ_{max}) occurred at 392 and 509 nm for PCzPDTQ and at 410 and 537 nm for PCzFDTQ. A 6–24 nm red-shift tendency was observed in the thin film compared to the solution because of an effective intermolecular interaction between the polymer chains at film formation [8]. Compared with PCzPDTQ, a long-wave absorption was observed in PCzFDTQ for either the solution or the thin film because the fused-phenyl ring of the dibenzophenazine derivative in PCzFDTQ increased the effective conjugation length by enhancing the planarity between the chain backbones [14]. In addition, the absorption spectra were more intense at 350–450 nm in PCzFDTQ because of an increase in a $\pi-\pi^*$ transition of the polymer backbone with the fused-phenyl ring structure [14,22]. The optical band gap energy of PCzPDTQ and PCzFDTQ calculated through the band edge were 2.06 and 1.97 eV, respectively [19,20].

The cyclic voltammograms of the PCzPDTQ and PCzFDTQ thin films, measured in 0.1 M tetrabutylammonium-hexafluorophosphate acetonitrile, are shown in Fig. 2(a). Table 2 contains the optical and

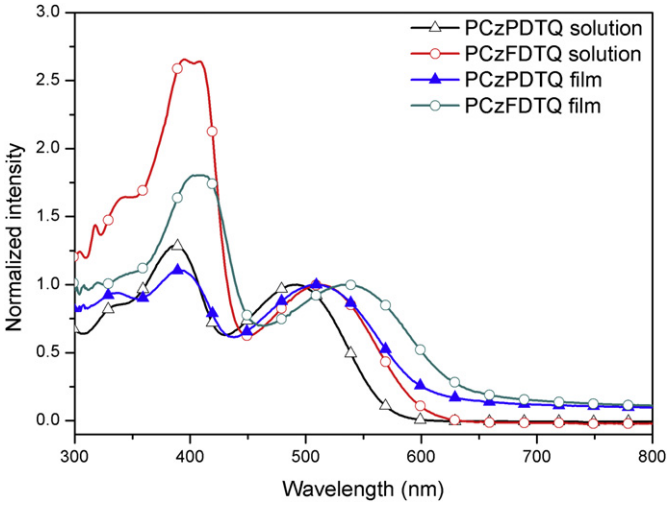

Fig. 1. Absorption spectra of polymer in solution & film.

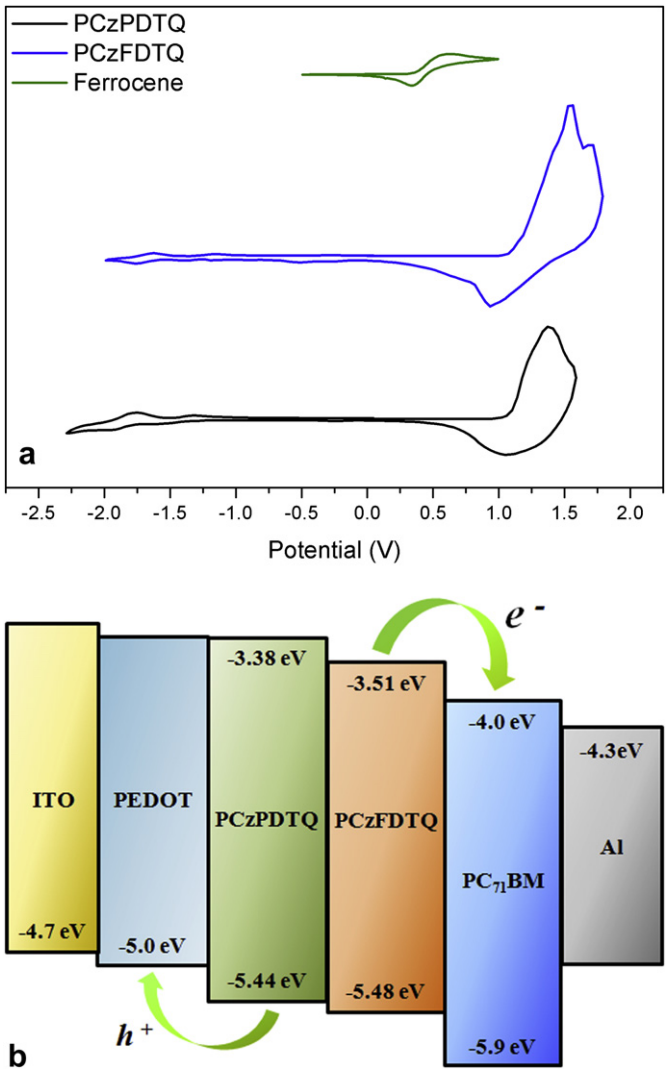

Fig. 2. Cyclic voltammogram & energy band diagram of polymers.

electrochemical properties of the polymers. As shown in Fig. 2 (a) and Table 2, the oxidation (E_{ox}^{onset}) onset potential values for PCzPDTQ and PCzFDTQ were +1.09 V and +1.13 V, respectively. The HOMO levels of PCzPDTQ and PCzFDTQ were −5.44 and −5.48 eV, respectively. The LUMO levels of PCzPDTQ and PCzFDTQ, calculated from the optical band gap energy from the HOMO levels, were - 3.38 and - 3.51 eV, respectively. Because all of the polymer HOMO levels are lower than the P3HT HOMO levels (4.9 eV), a relatively high air stability is expected [23]. In Fig. 2(b), the energy levels for ITO, PEDOT:PSS,

Table 2
Optical & electrochemical properties of the polymers.

Polymer	Absorption, λ_{max} (nm)		E_{ox}^{onset} (V)	E_{HOMO} (eV)[c]	E_{LUMO} (eV)[d]	E_{opt} (eV)[e]
	Solution[a]	Film[b]				
PCzPDTQ	386, 492	392, 509	1.09	−5.44	−3.38	2.06
PCzFDTQ	395, 513	410, 537	1.13	−5.48	−3.51	1.97

[a] Absorption spectrum in DCB solution (10^{-5} M).
[b] Spin-coated thin film (50 nm).
[c] Calculated from the oxidation onset potentials under the assumption that the absolute energy level of Fc/Fc+ was −4.8 eV below a vacuum.
[d] HOMO − Eopt.
[e] Estimated from the onset of UV–vis absorption data of the thin film.

PCzPDTQ, PCzFDTQ, $PC_{71}BM$ and Al are illustrated in a band diagram. Compared to the Density Functional Theory (DFT) prediction shown in Fig. 3, the HOMO and LUMO levels were lower. However, the HOMO and LUMO levels of PCzPDTQ and PCzFDTQ showed a similar tendency for both theoretical and measured values [15]. The energy level of the electrons (HOMO and LUMO) for PCzFDTQ was lower than PCzPDTQ because of the high oxidative stability of the fused-phenyl ring of PCzFDTQ. For the distribution of electrons in the LUMO level, in particular, the fused-phenyl ring of PCzFDTQ exhibited a higher electron distribution than the phenyl ring of PCzPDTQ because the fused-phenyl ring transports electrons with a higher conjugation length than the separated-phenyl ring.

As shown in Fig. 2(b), the difference of LUMO levels was the lowest with 0.49 eV between PCzFDTQ (−3.51 eV) and $PC_{71}BM$ (−4.0 eV), indicating that an effective electron transport is expected between PCzFDTQ and $PC_{71}BM$ [8,24].

To analyze the ordering structure of the polymers, X-ray diffraction in thin film was used, and the results are shown in Fig. 4(a). The out-of-plane peak, observed in all diffraction patterns with a highly ordered lamellar polymeric structure, did not occur.

In the (010) crystal plane related to π−π stacking, a broad diffraction peak of PCzPDTQ and PCzFDTQ was detected at approximately 21.7°, 23.5°. Using the calculation ($\lambda = 2d\sin\theta$), the π−π stacking distances (d_π) of PCzPDTQ and PCzFDTQ were 4.0 Å and 3.7 Å, respectively, indicating that the π−π stacking was somewhat effective in PCzFDTQ than in PCzPDTQ. This result of PCzPDTQ is similar to the benzene-thiophene aromatic system polymers that have perform well as OPVs [25].

According to a comparative analysis of the tilt angle through DFT calculations, as shown in Fig. 4(b), the tilt angle of the carbazole-thiophene linkage was 28°. The thiophene-quinoxaline of PCzPDTQ and thiophene-dibenzophenazine of PCzFDTQ were 19° and 47°, respectively. In terms of the tilt angle, PCzFDTQ was greater than PCzPDTQ. However, an effective π−π stacking is enabled in PCzFDTQ because the fused-phenyl ring (tilt angle: 0°) has strong planarity properties between the chain backbones. As shown in the XRD measurement in Fig. 4(a), PCzFDTQ had a shorter π−π stacking distance than PCzPDTQ. It appears that a high FF would occur in the

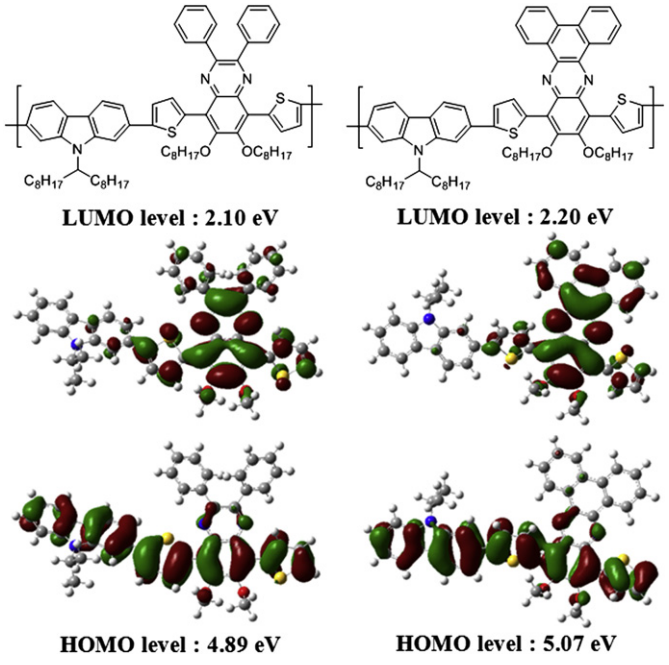

Fig. 3. DFT Gaussian simulation of polymers.

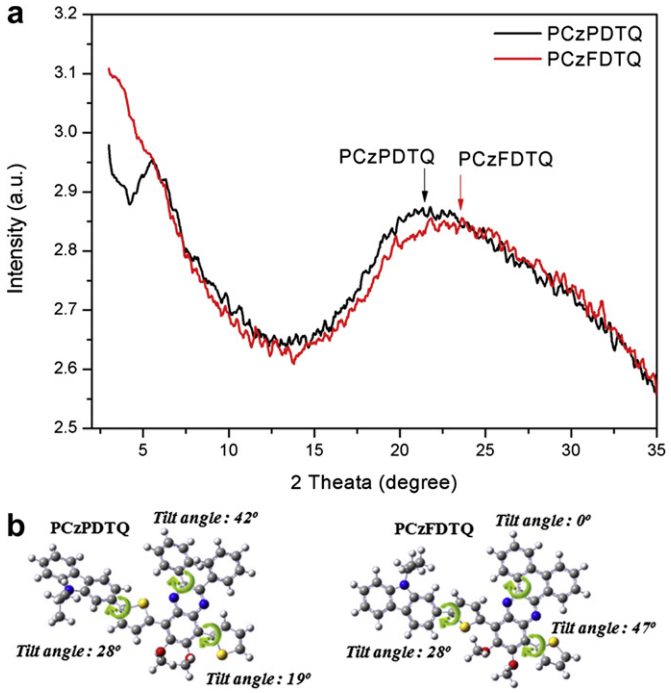

Fig. 4. X-ray diffraction pattern of polymers in thin film.

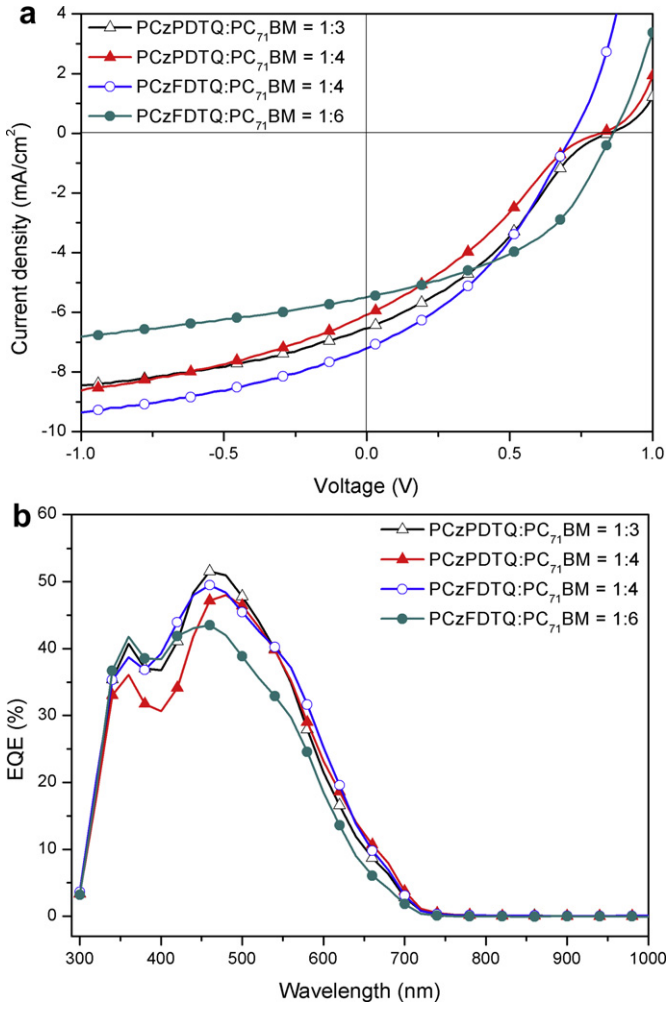

Fig. 5. (a) *J*–*V* characteristics & (b) EQE spectra of the BHJ solar cells with the device.

Table 3
Photovoltaic performance of the BHJ solar cells with the device.

Active layer (w/w)		Weight ratio (P:A, w/w)	V_{OC} (V)	J_{SC} (mA/cm^2)	FF (%)	PCE (%)
Polymer (P)	Acceptor (A)					
PCzPDTQ	$PC_{71}BM$	1:3	0.85	6.5	32.2	1.8
		1:4	0.81	6.0	29.2	1.4
PCzFDTQ	$PC_{71}BM$	1:3	0.65	6.2	36.2	1.5
		1:4	0.71	7.2	36.9	1.9
		1:5	0.83	5.7	42.4	2.0
		1:6	0.85	5.5	44.9	2.1

OPVs due to the close π−π stacking of PCzFDTQ with its planarity properties.

Fig. 5 and Table 3 show the results of the evaluation of the characteristics of the OPV devices. The device was structured as follows: ITO (170 nm)/PEDOT:PSS (40 nm)/active layer (50 nm)/BaF_2 (2 nm)/Ba (2 nm)/Al (100 nm). The active layer had an optimized blending ratio obtained by dissolving the polymer and phenyl-C71-butyric acid methyl ester ($PC_{71}BM$) in chlorobenzene (CB) with a concentration of approximately 0.5–1 wt% [20,26]. The open-circuit voltage (V_{OC}), short-circuit current (J_{SC}), fill factor (FF) and power conversion efficiency (PCE) were 0.85 V, 6.5 mA/cm^2, 32.2% and 1.8%, respectively, for PCzPDTQ with a 1:3 ratio of $PC_{71}BM$ (50 nm in thickness). However, device of PCzPDTQ: $PC_{71}BM$ (1:4 ratio) showed low performance, which is due to aggregation of $PC_{71}BM$ in part (see Fig. 5S). The structure of PCzPDTQ is similar with other qunoxaline polymer, but PCzPDTQ showed low PCE value compared to other quinoxaline polymer [14,15]. This result might be probably caused by a weakening of the electron accepting ability because their substitution with electron releasing octyloxy substituents was around polymer backbone.

For PCzFDTQ, the efficiency tended to improve with increasing $PC_{71}BM$. At a PCzFDTQ and $PC_{71}BM$ ratio of 1:6, the values of V_{OC}, J_{SC}, FF and PCE were 0.85 V, 5.5 mA/cm^2, 44.9% and 2.1%, respectively. While V_{OC} and J_{SC} were similar, the value of FF for PCzFDTQ increased by 39% compared to PCzPDTQ. As supported by the XRD data in Fig. 4, this increase was caused by the effects of the backbone planarity of the polymers. In other words, the effective π−π stacking found in PCzFDTQ with a high coplanarity increases the FF.

Both synthesized polymers had greater open circuit voltage values than P3HT (V_{oc} = 0.5–0.6) because of the lower HOMO levels. In other words, the HOMO level of the carbazole derivative introduced into the main chain of the polymers was low [23].

To check the accuracy of the device measurements, the External Quantum Efficiency (EQE) was measured and the EQE curve with the ratio of $PC_{71}BM$ shown in Fig. 5(b). In the EQE curve, photons mostly occurred in the polymer phase, correlating with the absorption spectra of the polymers [26]. As shown in Fig. 5(b), the EQE curve was similar to the UV–Vis spectra curve in Fig. 1. For PCzPDTQ, the short-circuit current density obtained from the EQE against $PC_{71}BM$ (1:3 ratio) was 6.6 mA/cm^2. For PCzFDTQ, the theoretical short-circuit current density obtained from the EQE against $PC_{71}BM$ (1:6 ratio) was 5.2 mA/cm^2. EQE of PCzPDTQ was more current value compared to that of PCzFDTQ, which is due to high molecular weight of PCzPDTQ (31.0 kg/mol) compared to molecular weight PCzFDTQ (12.3 kg/mol).

The AFM of the polymer/PCBM blend films are shown in Fig. 6. As observed in Fig. 6(a), a smooth morphology appeared when PCzPDTQ and $PC_{71}BM$ were blended in a 1:3 ratio with root-mean-

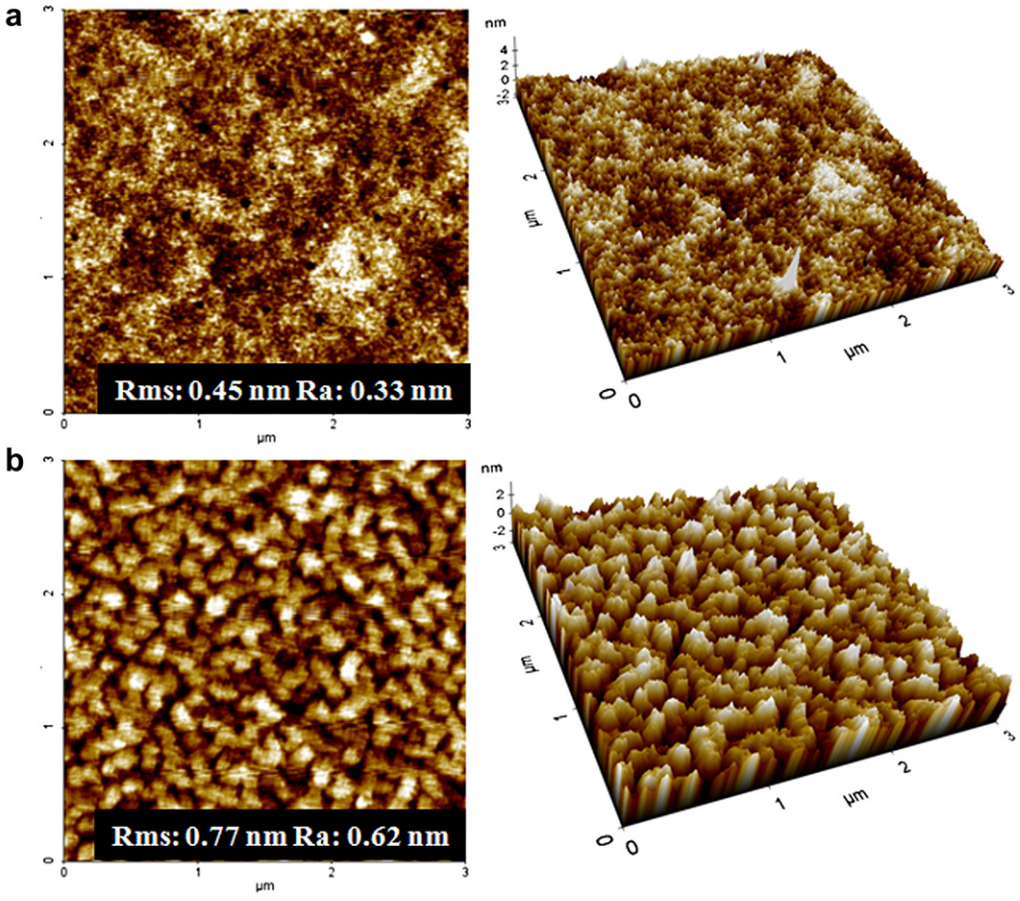

Fig. 6. Topographic AFM images of (a) PCzPDTQ: $PC_{71}BM$ 1:3 (3 × 3 μm^2) (b) PCzFDTQ:$PC_{71}BM$ 1:6 (3 × 3 μm^2).

square roughness (Rms) of 0.45 nm. Compared with PCzPDTQ, a large-phase separation was observed when PCzFDTQ and $PC_{71}BM$ were mixed at a 1:6 ratio with Rms of 0.77 nm, as shown in Fig. 6(b). In addition, macro p-n channels were formed. The large-phase separation produces a low photocurrent by reducing the charge separation and increasing the exciton diffusion length and the recombination of electric charges [27]. The blend film between PCzPDTQ and $PC_{71}BM$ should demonstrate good film morphology with a smaller domain size approaching the ideal domain size of about 10 nm [28], which showed high EQE value compared to the blend film between PCzFDTQ and $PC_{71}BM$. The lowest photocurrent (5.5 mA/cm^2) was observed for a PCzFDTQ/$PC_{71}BM$ ratio of 1:6. Conversely, FF improved by 39% due to the superior π–π stacking coplanarity. As a result, PCzFDTQ had a relatively higher efficiency than PCzPDTQ.

4. Conclusions

In this study, two new acceptor units, in which octyloxy with a high solubility was introduced, have been synthesized. In addition, D–A type polymers, PCzPDTQ, which accepted carbazole derivatives as a donor, and PCzFDTQ were polymerized. Both PCzPDTQ and PCzFDTQ showed high solubility, thermal stability and a low-band gap. According to XRD measurements, the π–π stacking distance (d_π) of PCzPDTQ and PCzFDTQ were 4.4 and 4.3 Å, respectively. With a large-phase separation, the J_{SC} of PCzFDTQ was lower than PCzPDTQ. With the superior coplanarity of the fused phenyl rings, the FF of PCzFDTQ was 39% higher than PCzPDTQ. Continued optimization of the chemical structures and the device structure of the polymers may further improve the polymer performances, becoming more effective.

Acknowledgments

This research was supported by a grant from the Fundamental R&D Program for Core Technology of Materials funded by the Ministry of Knowledge Economy, Republic of Korea. This work was supported by the National Research Foundation of Korea Grant funded by the Korean Government (MEST) (NRF-2009-C1AAA001-2009-0093526).

Appendix A. Supplementary data

Supplementary data related to this article can be found at http://dx.doi.org/10.1016/j.polymer.2012.10.056.

References

[1] Friend RH, Gymer RW, Holmes AB, Burroughes JH, Marks RN, Taliani C, et al. Nature 1999;397(2):121–8.
[2] Lu W, Kuwabara J, Kanbara T. Macromolecules 2011;44(6):1252–5.
[3] Song HJ, Lee JY, Song IS, Moon DK, Haw JR. J Ind Eng Chem 2011;17(2):352–7.
[4] Wu W, Ye S, Tang R, Huang L, Li Q, Yu G, et al. Polymer 2012;53(15):3163–71.
[5] Iwan A, Palewicz M, Chuchmala A, Gorecki L, Sikora A, Mazurek B, et al. Synth Met 2012;162(1):143–53.
[6] Lee JY, Kim SH, Song IS, Moon DK. J Mater Chem 2011;21(41):16480–7.
[7] Mondal R, Ko S, Verploegen E, Becerril AH, Toney MF, Bao Z. J Mater Chem 2011;21(5):1537–43.
[8] Zhang J, Cai W, Huang F, Wang E, Zhong C, Liu S, et al. Macromolecules 2011; 44(4):894–901.
[9] Dong Y, Cai W, Hu X, Zhong C, Huang F, Cao Y. Polymer 2012;53(7):1465–72.
[10] Manceau M, Angmo D, Jørgensen M, Krebs FC. Org Electron 2011;12(4):566–74.
[11] Krebs FC, Fyenbob J, Jørgensen M. J Mater Chem 2010;20(41):8994–9001.
[12] Yamamoto T, Kokubo H, Kobashi M, Sakai Y. Chem Mater 2004;16(23):4616–8.
[13] Yasuda T, Sakai Y, Aramaki S, Yamamoto T. Chem Mater 2005;17(24):6060–8.
[14] Lee YK, Nam YM, Jo WH. J Mater Chem 2011;21(23):8583–90.
[15] Blouin N, Michaud A, Gendron D, Wakim S, Blair E, Rodica NP, et al. J Am Chem Soc 2008;130(2):732–42.
[16] Lai MH, Chueh CC, Chen WC, Wu JL, Chen FC. J Polym Sci Part A Polym Chem 2007;45(5):973–85.
[17] Tsai JH, Chueh CC, Lai MH, Wang CF, Chen WC, Ko BT, et al. Macromolecules 2009;42(6):1897–905.
[18] Zhang Y, Zou J, Yip HL, Chen KS, Zeigler DF, Sun Y, et al. Chem Mater 2011; 23(9):2289–91.
[19] Qin R, Li W, Li C, Du C, Veit C, Schleiermacher HF, et al. J Am Chem Soc 2009; 131(41):14612–3.
[20] Yi H, Al-Faifi S, Iraqi A, Watters DC, Kingsleyb J, Lidzey DG. J Mater Chem 2011; 21(35):13649–56.
[21] Song HJ, Lee SM, Lee JY, Choi BH, Moon DK. Synth Met 2011;161(22):2451–659.
[22] Yang R, Tian R, Yan J, Zhang Y, Yang J, Hou Q, et al. Macromolecules 2005; 38(2):244–53.
[23] Hou J, Chen TL, Zhang S, Huo L, Sista S, Yang Y. Macromolecules 2009;42(23): 9217–9.
[24] Jiang JM, Yang PA, Hsieh TH, Wei KH. Macromolecules 2011;44(23):9155–63.
[25] Lu G, Usta H, Risko C, Wang L, Facchetti A, Ratner MA, et al. J Am Chem Soc 2008;130(24):7670–85.
[26] Gadisa A, Mammo W, Andersson LM, Admassie S, Zhang F, Andersson MR, et al. Adv Funct Mater 2007;17(18):3836–42.
[27] Wang E, Hou L, Wang Z, Ma Z, Hellstrom S, Zhuang W, et al. Macromolecules 2011;44(7):2067–73.
[28] Frechet JMJ, Thompson BC. Angew Chem 2008;47(1):58–77.